NeuroImage: Clinical 31 (2021) 102756

Contents lists available at ScienceDirect

NeuroImage: Clinical

journal homepage: www.elsevier.com/locate/ynicl

Brain perfusion imaging in neonates

Jérôme Baranger [a,b], Olivier Villemain [a,b,c], Matthias Wagner [d], Mariella Vargas-Gutierrez [e], Mike Seed [a,b,g], Olivier Baud [f], Birgit Ertl-Wagner [d], Julien Aguet [g,*]

[a] Department of Pediatrics, Labatt Family Heart Centre, The Hospital for Sick Children, Toronto, Ontario, Canada
[b] Translation Medicine Department, SickKids Research Institute, Toronto, Ontario, Canada
[c] Department of Medical Biophysics, University of Toronto, Toronto, Canada
[d] Department of Diagnostic Imaging, Division of Neuroradiology, The Hospital for Sick Children, Toronto, Canada
[e] Department of Critical Care Medicine, The Hospital for Sick Children, Toronto, ON, Canada
[f] Division of Neonatology and Pediatric Intensive Care, Children's University Hospital of Geneva and University of Geneva, Geneva, Switzerland
[g] Department of Diagnostic Imaging, The Hospital for Sick Children, Toronto, Canada

ARTICLE INFO

Keywords:
Brain
Pediatrics
Perfusion
MRI
Ultrasound

ABSTRACT

Abnormal variations of the neonatal brain perfusion can result in long-term neurodevelopmental consequences and cerebral perfusion imaging can play an important role in diagnostic and therapeutic decision-making. To identify at-risk situations, perfusion imaging of the neonatal brain must accurately evaluate both regional and global perfusion. To date, neonatal cerebral perfusion assessment remains challenging. The available modalities such as magnetic resonance imaging (MRI), ultrasound imaging, computed tomography (CT), near-infrared spectroscopy or nuclear imaging have multiple compromises and limitations. Several promising methods are being developed to achieve better diagnostic accuracy and higher robustness, in particular using advanced MRI and ultrasound techniques.

The objective of this state-of-the-art review is to analyze the methodology and challenges of neonatal brain perfusion imaging, to describe the currently available modalities, and to outline future perspectives.

1. Introduction

Cerebral blood flow in neonates can be compromised due to a variety of clinical conditions. Prematurity, perinatal asphyxia, and various congenital heart defects are common, but not exhaustive examples (Greisen, 2005). Impaired cerebral perfusion can lead to disorders of neurocognitive development and subsequent disabilities that may reach well into adulthood, making it a major public health concern. The development of neonatal perfusion imaging methods could have a major impact on perinatal medicine by enabling a timely and precise diagnosis of cerebral at-risk situations. Various fundamentally different technologies currently exist to image and quantify brain perfusion. For magnetic resonance imaging (MRI), these encompass contrast-enhanced perfusion methods including T1-weighted dynamic contrast-enhanced and dynamic susceptibility contrast techniques, as well as arterial spin labelling (ASL) and intravoxel incoherent motion (IVIM) MRI. Ultrasound techniques include the assessment of the pre-cranial arteries with conventional ultrasound and more recently full brain perfusion assessment by ultrafast ultrasound imaging (UUI). Further perfusion imaging techniques comprise conventional single photon emission computed tomography (SPECT), positron emission tomography (PET) techniques, computed tomography perfusion, and near-infrared spectroscopy. Nuclear medicine and computed tomography (CT) based techniques have an inherent exposure to ionizing radiation (Brody et al., 2007; Kleinerman, 2006), which is a particular concern in neonates. Contrast-enhanced techniques require intravenous (IV) access and exogenous contrast agent administration. For CT, iodine-based contrast is used, and the associated risks include contrast-induced nephrotoxicity essentially

Abbreviations: ASL, Arterial Spin Labelling; CBF, Cerebral Blood Flow; CBV, Cerebral Blood Volume; CEUS, Contrast Enhanced Ultrasound; CT, Computed Tomography; EEG, Electroencephalogram; FDG, 2-Deoxy-2[18F]-Fluoro-D-Glucose; HD, High-Density; HIE, Hypoxic-Ischemic Encephalopathy; IV, Intravenous; IVIM, Intravoxel Incoherent Motion; MRI, Magnetic Resonance Imaging; NIRS, Near-Infrared Spectroscopy; PET, Positron Emission Tomography; RI, Resistivity Index; SNR, Signal-To-Noise Ratio; SPECT, Single Photon Emission Computed Tomography; T1w, T1-weighted imaging; T2w, T2-weighted imaging; T2*, gradient echo T2 weighted imaging; UUI, Ultrafast Ultrasound Imaging.

* Corresponding author.
E-mail address: julien.aguet@sickkids.ca (J. Aguet).

https://doi.org/10.1016/j.nicl.2021.102756
Received 5 November 2020; Received in revised form 21 June 2021; Accepted 3 July 2021
Available online 14 July 2021

when kidney function is impaired and allergic reactions of various degree of severity (Davenport et al., 2021). For MRI, gadolinium-based contrast is used, and aside from rare and often mild allergic reactions, there is a rare risk of nephrogenic systemic fibrosis (Davenport et al., 2013; Nardone et al., 2014). Recent reports have described gadolinium deposits in the brain, of which the significance is not yet fully understood (Young et al., 2018). Thus, there is a need for non-invasive perfusion imaging methods that do not involve ionizing radiation, especially in the particularly vulnerable neonatal population. With the recent advent of UUI introducing both high spatial and temporal resolution to Doppler imaging, quantitative analysis down to a microvascular level at the patient's bedside has become conceivable (Demene et al., 2019). In this review, we provide an overview of the current state-of-the-art in brain perfusion imaging in neonates and summarize the current practices and future developments.

2. Physiological considerations of neonatal brain perfusion

The brain comprises a vascular network reigned by a complex regulatory system which is designed to maintain a stable blood perfusion in order to ensure the integrity and functionality of cerebral tissue. Cerebral blood flow (CBF) is expressed in units of milliliters per 100 g of brain tissue per minute. Multiple intrinsic and extrinsic factors influence this parameter such as intravascular and intracranial pressure, hematocrit levels and arterial gases such as carbon dioxide and oxygen.

Understanding the normal transition of cerebral perfusion from the fetal to the perinatal period and the physiologic brain maturation is essential to correctly image and quantify changes in perfusion induced by pre-, peri- and post-natal brain injury (De Vis et al., 2013).

One of the key mechanisms of cerebral perfusion is autoregulation. Cerebral autoregulation is the ability of brain to maintain a constant blood flow during normal variations of blood pressure, for instance due to a change in position, strain, or stress. Autoregulation is not an all-or-none phenomenon. The flow-pressure curve generally exhibits a plateau usually with a small positive slope. Its range and the position of its thresholds may vary. Autoregulation is therefore sometimes also called pressure-flow reactivity. This mechanism should not be confused with neurovascular regulation which occurs to match blood flow to the metabolic needs during functional activation. In spite of considerable research efforts, the characteristics of autoregulation in neonates is still not well defined and only sparse data in the literature link abnormal blood pressure to brain injury, brain damage or neurodevelopmental deficit. By contrast, there is strong evidence supporting a robust and clinically significant relation between the partial pressure of carbon dioxide and CBF. There is also a significant association between hyperventilation and hypocapnia on the one hand and between brain damage and cerebral palsy on the other. (Greisen and Vannucci, 2001).

The imaging techniques presented below exploit these physiological (or pathophysiological) parameters to better understand CBF and its variations in neonates.

3. Imaging techniques to assess CBF in neonates (Graphical ABSTRACT)

3.1. Magnetic resonance imaging (MRI)

There are various different MRI perfusion methods, which are based on different pulse sequences. These techniques utilize either exogenous or endogenous contrast agents to assess both regional and global cerebral perfusion.

3.1.1. Dynamic susceptibility contrast MRI perfusion

Dynamic susceptibility contrast perfusion relies on the susceptibility-induced signal loss seen on conventional T2 weighted (T2w) or gradient echo T2 weighted (T2*w) images during the first pass of an exogenous intravenously administered paramagnetic, Gadolinium-based contrast agent (Ostergaard, 2005). Hemodynamic changes are assessed both on a global and regional level and expressed as mean transit time, time to peak and cerebral blood volume (CBV) which in turn are used to calculate CBF (Ostergaard, 2005). Color maps of these quantitative measurements can be obtained (Essig et al., 2013; Petrella and Provenzale, 2000) (Fig. 1). Applying this technique to the neonate has proven difficult on various levels and only few studies exist (Tanner et al., 2003; Wintermark et al., 2008a, 2008b). When studying the healthy newborn, administration of contrast agents is difficult to justify. Imaging the neonatal brain with MRI usually does not require contrast-enhanced sequences for diagnostic completeness. Considering the potential repeated exposures to Gadolinium-based contrast agent and the growing controversy around the potential risk of cerebral gadolinium deposition, alternative, non-contrast-enhanced methods for MRI perfusion should always be considered (Harvey et al., 2020; Kanda et al., 2014, 2015; Young et al., 2018). If contrast administration is absolutely required, manual injections are usually preferred over automated power injectors to avoid potential contrast agent extravasation or jeopardizing intravenous (IV) access, since access usually consists of small caliber catheters often positioned on the hands or feet in pediatric patients (ACR–ASNR–SPR, 2017).

3.1.2. Dynamic contrast-enhanced MRI perfusion

Dynamic contrast enhanced perfusion relies on the Gadolinium-based contrast agent effect of T1 relaxation time shortening resulting in a signal increase. By injecting a bolus of Gadolinium-based contrast agent, the enhancement pattern of a region of interest can be studied over time by acquisition of baseline images without contrast followed by rapid succession of repeated T1-weighted imaging (T1w). The regional accumulation of Gadolinium-based contrast agent within the blood vessels as well as the fraction of Gadolinium-based contrast agent which has diffused into the extravascular, extracellular space will result in an increase in signal due to the T1 shortening. Dynamic contrast enhanced perfusion MRI assesses tissue perfusion properties on a microvascular level (Gaddikeri et al., 2016; Paldino and Barboriak, 2009). Through pharmacokinetic modeling, parameters reflecting capillary permeability, regional blood volume and regional blood flow can be measured. Use of dynamic contrast enhanced MRI has been primarily described in imaging of tumors and peripheral vascular system (Gordon et al., 2014). As with dynamic susceptibility contrast perfusion MRI, use of an IV access for the administration of an exogeneous contrast agent are required, both of which come with their inherent risks and limitations for the neonate as previously described.

3.1.3. Phase-Contrast MRI

Phase-contrast MRI allows for quantitative imaging of moving fluids based on the principle that spins moving along a magnetic field gradient develop a phase shift which is proportional to their velocity. By analysing the phase information within a transverse section of a given vessel of interest, velocity can be calculated for each voxel and a phase contrast image is obtained (Fig. 2). Post-processing software then allows to quantify this velocity and draw a flow curve, e.g. for a complete cardiac cycle (Lotz et al., 2002). When applying this principle at the level of the extracranial, pre-cerebral arteries including the internal carotid arteries and the vertebral arteries, total cerebral blood flow can be reliably measured (Spilt et al., 2002). Brain volume is measured by segmentation of isotropic 3D sequences with a high spatial resolution (Prsa et al., 2014; Werner et al., 2010). Mean total CBF is then calculated by dividing total blood flow by brain volume. Applied to preterm and term neonates, total CBF measured using phase-contrast MRI was shown to be significantly correlated to postconceptional age and weight, supporting the utility of such a non-invasive technique for measuring total CBF in the newborn (Benders et al., 2011). This technique, however, only provides an estimate of the mean global CBF and does not offer information on regional CBF. Phase contrast MRI is already common practice in neonatal cardio-vascular imaging (Kellenberger et al., 2007). Motion

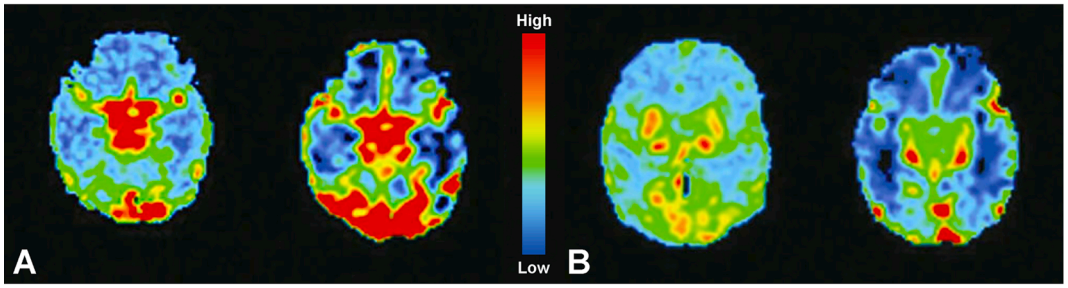

Fig. 1. Dynamic susceptibility contrast MRI Perfusion. Panels A and B show perfusion maps with CBF on the left and CBV on the right of each panel, at two different levels to illustrate marked hyperperfusion in the occipital lobes (A), basal ganglia (B) and motor cortex (A and B) reflective of basal ganglia injury pattern. Adapted and with permission from Wintermark et al. (Wintermark et al., 2008a).

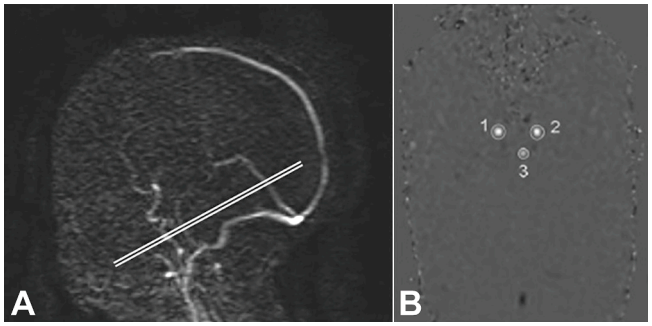

Fig. 2. Phase Contrast MRI. Sagittal 2D phase contrast image (A) to illustrate the positioning of the axial 2D phase contrast image showing in plane flow signal intensity within the internal carotid arteries (B: 1 and 2) and the basilary artery (B: 3). Adapted and with permission from Benders et al. (Benders et al., 2011).

artifacts, flow turbulences and magnetic field inhomogeneities, however, significantly influence the accuracy of measurements (Hofman et al., 2019; Lotz et al., 2002).

3.1.4. *Arterial spin labeling (ASL) MRI perfusion*

While dynamic susceptibility contrast and dynamic contrast enhanced MRI perfusion techniques require the administration of an exogenous contrast agent, arterial spin labeling utilizes an inherent endogenous contrast agent, blood water molecules. Prior to the labeling process an image is acquired for background magnetization within the brain. Arterial blood water is then labeled by selectively inverting the magnetization of arterial blood water spins circulating into the brain at the level of the neck which are imaged at the level of the brain after a short transit time (Fig. 3). Subtraction of the two images generates a perfusion-weighted image (Ferre et al., 2013). Quantification of CBF (in units of mL/100 g of brain tissue/min) with ASL is based on mathematical models using time-averaged signal intensities in the background magnetization and arterial spin labeled images (Alsop et al., 2015; Varela et al., 2015).

The brain weight is estimated from segmentation of acquired anatomical 3D sequences (Ferre et al., 2013). Both regional and global cerebral perfusion can be studied. Several labeling methods exist, of which pseudo-continuous labeling was shown to be more accurate in neonates, achieving superior image quality by improving labeling efficiency and signal-to-noise ratio (SNR) compared to other methods (Alsop et al., 2015; Boudes et al., 2014; Wu et al., 2011).

As it avoids intravenous administration of an exogenous contrast agent and ionizing radiation, ASL is an appealing method for brain perfusion imaging in the neonate (Miranda et al., 2006). When motion artifacts under a feed and sleep technique hinder assessment, the sequence can be repeated (Antonov et al., 2017; Windram et al., 2012). Several studies have demonstrated the feasibility of ASL in neonates and young infants (Biagi et al., 2007; De Vis et al., 2013; Duncan et al., 2014; Jain et al., 2012; Massaro et al., 2013; Miranda et al., 2006; Pienaar et al., 2012; Varela et al., 2015). Reference values have been established

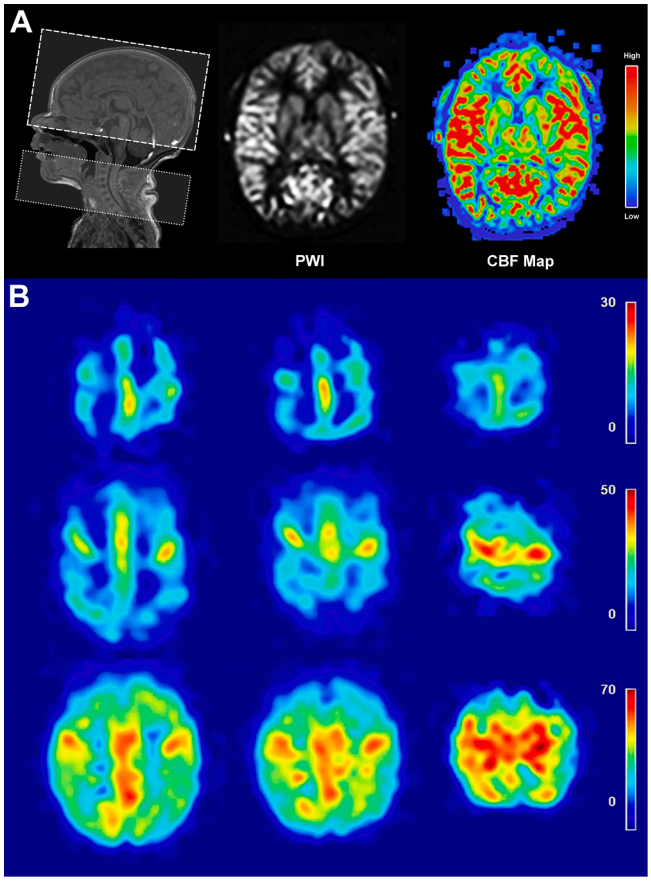

Fig. 3. Arterial Spin Labeling (ASL) MRI. A: Magnetization of arterial blood water spins within the pre-cerebral arteries is inverted by applying a radio-frequency pulse (left, dotted box), followed by a short delay during which the spins reach the brain circulation where a "labelled" image is obtained. Prior background magnetization is captured within the same field of view (left dashed box). Subtraction of the two images generates a perfusion-weighted image (PWI). Quantification of CBF (in units of mL/100 g of brain tissue/min) with ASL is based on mathematical models using time-averaged signal intensities in the background magnetization and arterial spin labeled images. B: ASL perfusion images representing CBF in three infants born at 25 weeks gestational age (top row), 31 weeks gestational age (middle row) and scanned 40 weeks gestational age (bottom row). Perfusion increases within the central sulcus with gestational age (middle row) and is more homogeneously spread in a term newborn (bottom row). Adapted and with permission from De Vis et al. (De Vis et al., 2013).

in healthy subjects aged between 6 months to 15 years (Carsin-Vu et al., 2018).

3.1.5. Intravoxel incoherent motion (IVIM) MRI perfusion

Diffusion-weighted MRI assesses the random movement of individual water molecules within tissue. Every molecule possesses a thermal energy which induces motion resulting in collisions with other molecules, and resultant changes in their direction of motion. Within a magnetic field with applied encoding gradient pulses, signal attenuation is observed secondary to diffusivity, which increases with the degree of field gradient encoding, commonly known as the b value in diffusion-weighted MRI (Le Bihan, 2019).

First described by Le Bihan et al. in conjuncture with the concept of diffusion in 1986 (Le Bihan et al., 1986), collective motion of water molecules within a network of randomly oriented capillaries equals blood flow and is termed "pseudodiffusion" (Le Bihan, 2019). Derived from the Stokes-Einstein equation, pseudodiffusion is expressed as a coefficient depending on a mean capillary segment length and the mean velocity within. Both diffusion and pseudodiffusion contribute to the signal decay resulting in a biexponential signal decay curve given a ten times faster signal decay of pseudodiffusion at low b values. This deviation is called the IVIM effect. Obtained signal attenuation data is then processed via mathematical algorithms which are beyond the scope of this review. Le Bihan and Turner have shown how IVIM parameters can be related to conventional perfusion parameters based on two important variables: the capillary segment length and the total capillary length (Le Bihan and Turner, 1992). Considering that these two lengths are constant for a given tissue, a relative perfusion or blood flow can be estimated from the product of $D^*.f_{IVIM}$ where D^* is the pseudodiffusion and f_{IVIM} the flowing blood fraction (Fig. 4).

Microvascular perfusion has been studied primarily in tumor imaging to date, both on a global and on a regional level (Stieb et al., 2016).

IVIM-based MRI perfusion provides information on both tissue microcirculation and blood flow within a single sequence and does not require the administration of a contrast agent, which makes it an appealing concept for neonatal imaging. A recent study has shown its potential in perfusion and diffusion imaging of the developing human fetus (Jakab et al., 2017).

3.2. Ultrasonography

Ultrasonography of the neonatal brain utilizes the naturally available anatomical windows through the anterior and when possible, posterior fontanels, thin temporal bone, and mastoid bone. With its widespread availability, lack of exposure to ionizing radiation and no need for sedation, ultrasonography allows for a bedside evaluation of the neonatal brain. However, compliance with a standardized imaging protocol, knowledge of the hardware and user expertise is required in order to achieve acceptable reproducibility (Dudink et al., 2020). Several approaches exist to estimate cerebral perfusion.

3.2.1. Conventional Doppler

The so-called Doppler ultrasound modes use the Doppler effect which is defined by the shift in frequency of a sound wave due to a reflector, i.e., blood cell, moving toward or away from an object, i.e., transducer. In particular, spectral Doppler (or Pulse-Wave Doppler) ultrasonography uses a Fourier analysis to average these frequencies over a defined time period, converts them to velocities and displays the spectrum of frequencies as a waveform (Pellett and Kerut, 2004; Rubin, 1994). Total CBF has been estimated using the intravascular flow

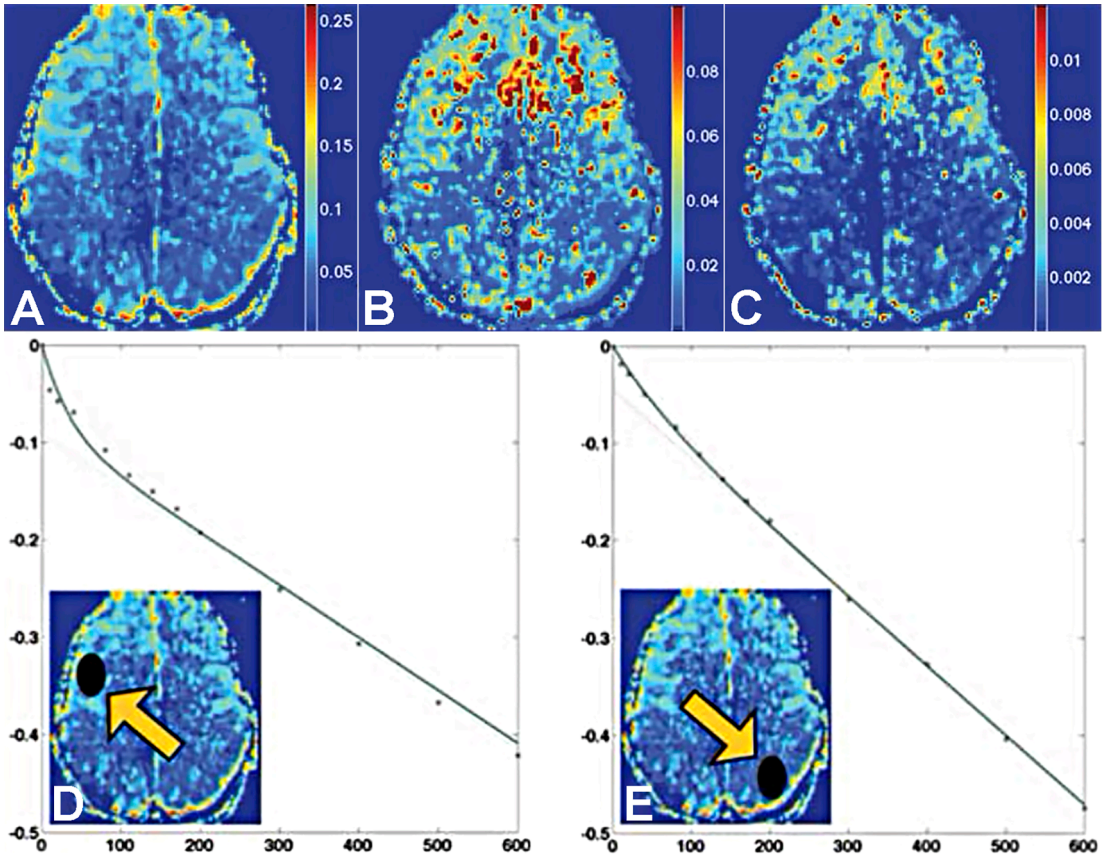

Fig. 4. Intravoxel Incoherent Motion (IVIM) MRI Perfusion. IVIM parameters f_{IVIM} (A), D^* (B) and $D^*.f_{IVIM}$ (C) reflect hyperperfusion in both frontal lobes, predominately on the right. Signal intensity decay as function of b with corresponding biexponential fit are represented for a region of interest within the hyperperfused right frontal lobe (D) and within a left parietal control region (E). Adapted and with permission from Federau et al. (Federau et al., 2014).

volume calculated with angle-corrected time-averaged velocities and vessel cross-sectional area within the extracranial internal carotid and vertebral arteries (Ehehalt et al., 2005). The accuracy of this approach relies on the precise measurement of small luminal diameters (less than 2 mm for the vertebral arteries), choosing an optimal insonation angle and correct estimation of the time-averaged velocity as even small errors result in significant changes (Ehehalt et al., 2005; Ranke et al., 1992). The obtained information on pre-cerebral blood flow informs only on a global intra-cerebral scale and cannot demonstrate regional changes. Other common ultrasound Doppler tools include Color Doppler and Power Doppler. While Color Doppler exhibits a lack of sensitivity to slow blood flows, Power Doppler is proportional to the CBV (Rubin et al., 1995) and is more sensitive to microvascular flow. It can be used to study the regional cerebral perfusion in neonates in cortical or deep structure such as the basal ganglia (Heck et al., 2012) (Fig. 5). The aforementioned proportional law between CBV and Power Doppler depends on several parameters, including sound attenuation and the geometry and elevation thickness of the ultrasound beam. Therefore, within a given pixel, Power Doppler is said to represent the fractional moving blood volume and is provided in relative units (% or dB) (Rubin et al., 1995). Therefore, Power Doppler is more suitable for relative measurements between areas or time points rather than for quantitative CBV measurements.

3.2.2. *Dynamic tissue perfusion measurement*

Dynamic tissue perfusion measurement quantifies mean perfusion intensity (expressed in cm/s) within a chosen region of interest from a color doppler video clip acquired over the length of at least one cardiac cycle (Scholbach, 2009, 2008) (Fig. 6). This method has been recently applied to retrospectively study perfusion of the basal ganglia in a small population of infants treated with therapeutic whole body hypothermia for hypoxic-ischemic encephalopathy (HIE) (Faingold et al., 2016). As with other conventional ultrasound methods, dynamic tissue perfusion measurement requires a standardized approach of chosen regions of interest and allows only for a regional analysis of mean perfusion intensity quantification. Comparison to other more widely used quantitative parameters such as CBF is challenging as dynamic tissue perfusion measurement does not account for tissue volume.

3.2.3. *Contrast enhanced ultrasound (CEUS)*

CEUS aims to increase intravascular echogenicity by injecting an ultrasound contrast agent: phospholipid membrane encased gas microbubbles which compress and expand in a non-linear fashion when subjected to an ultrasound beam. The resulting increased echo signal creates an intravascular contrast similar in principle to cross-sectional imaging utilizing intravascular contrast-agents (Fig. 7).

Its use in neonates has been limited. While it was considered contraindicated for patients with cardiac shunts until 2016, ultrasound contrast agents have proven to be safe and efficient over the years (Appis et al., 2015). The use of ultrasound contrast agents is still off-label for brain ultrasonography and requires parental consent. CEUS could be advantageous over MRI in terms of required infrastructure, transport, support personnel and costs. There is, however, currently little data supporting routine use of ultrasound contrast in neonatal brain imaging (Hwang, 2019). The technique has recently been used to examine neonates with suspected HIE and was shown to be qualitatively comparable to MRI perfusion maps (Hwang et al., 2019). Comparison of quantifiable data to established MRI and CT perfusion techniques is required in order to establish this technique as a valuable alternative or complementary technique. Performance, interpretation, and data post-processing also

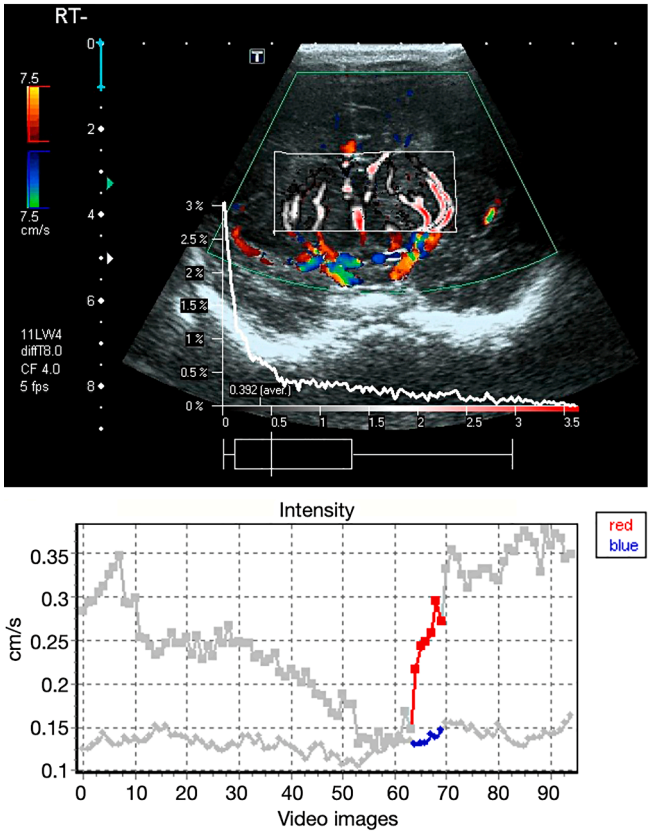

Fig. 6. Dynamic tissue perfusion measurement. A region of interest is selected within the basal ganglia on a color Doppler ultrasound clip acquired during at least one cardiac cycle to quantify mean perfusion intensity (in cm/s) shown on the intensity curve at the bottom in a 1-day-old patient diagnosed with hypoxic-ischemic encephalopathy. Adapted and with permission from Faingold et al. (Faingold et al., 2016).

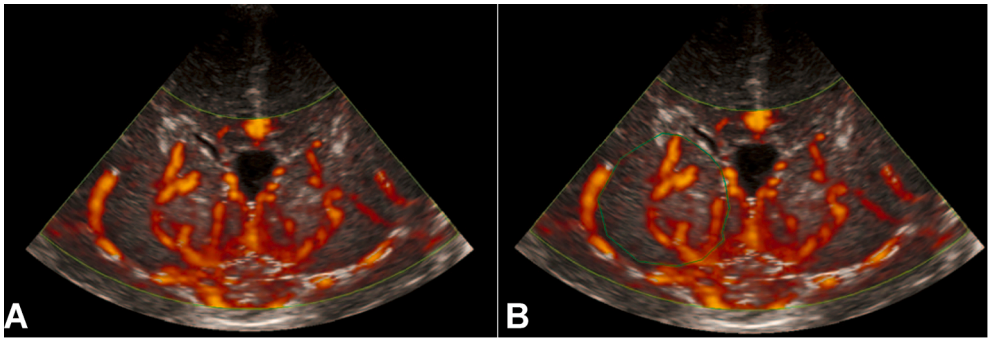

Fig. 5. Conventional Doppler Ultrasound. Power Doppler flow mapping overlayed on a b-mode coronal view of the basal ganglia and anterior horns of the lateral ventricles including the middle cerebral arteries. Regional vascularity is measured during post-processing by counting the number and strength of colour pixels in a preselected region. Adapted and with permission from Heck et al. (Heck et al., 2012).

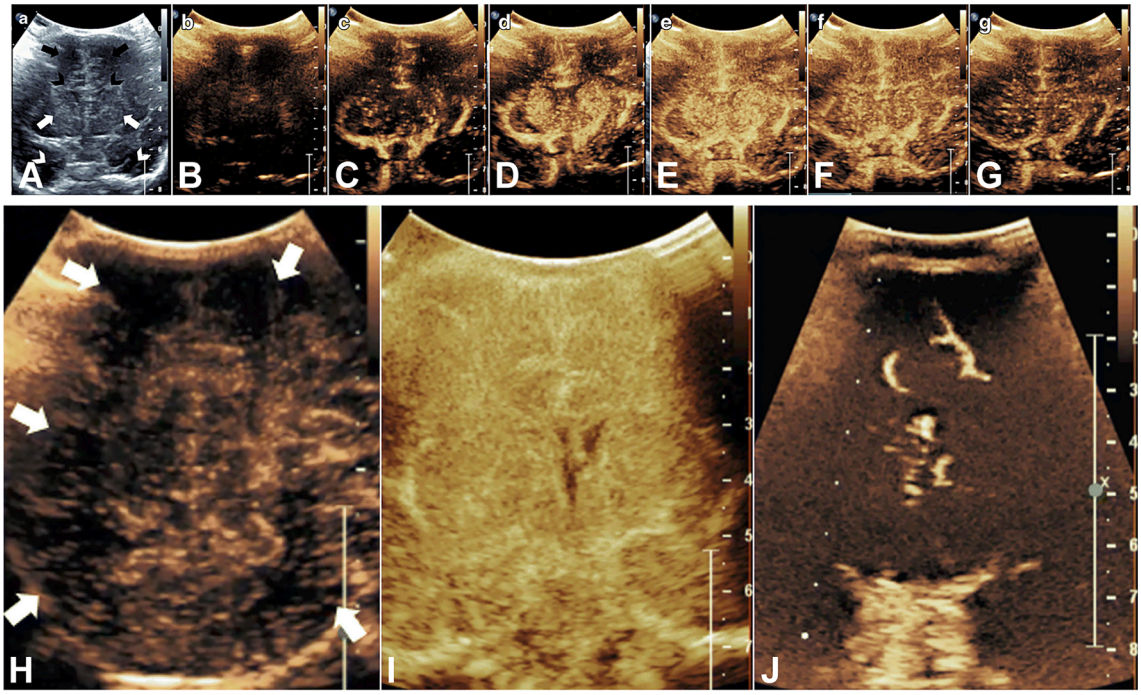

Fig. 7. Contrast-enhanced Ultrasound (CEUS). A: Mid-coronal b-mode image showing bilateral frontal lobes (black arrows), frontal horns of the lateral ventricles (black chevrons), basal ganglia (white arrows), and temporal lobes (white chevrons). B-G: Static images of a dynamic microbubble wash-in on mid-coronal views of a healthy neonate. H: Posterior parietooccipital view in a neonate with hypoxic-ischemic injury showing diffuse hypoperfusion with multiple areas of paucity of microbubbles (white arrows), reflecting perfusion abnormalities. I: Coronal view through the basal ganglia in a neonate with diffuse hypoxic-ischemic injury, in the immediate post-injury period, showing diffuse hyperperfusion. J: Coronal view through the basal ganglia in an infant following prolonged cardiac arrest, showing diffuse hypoperfusion. Adapted and with permission from Hwang (Hwang, 2019).

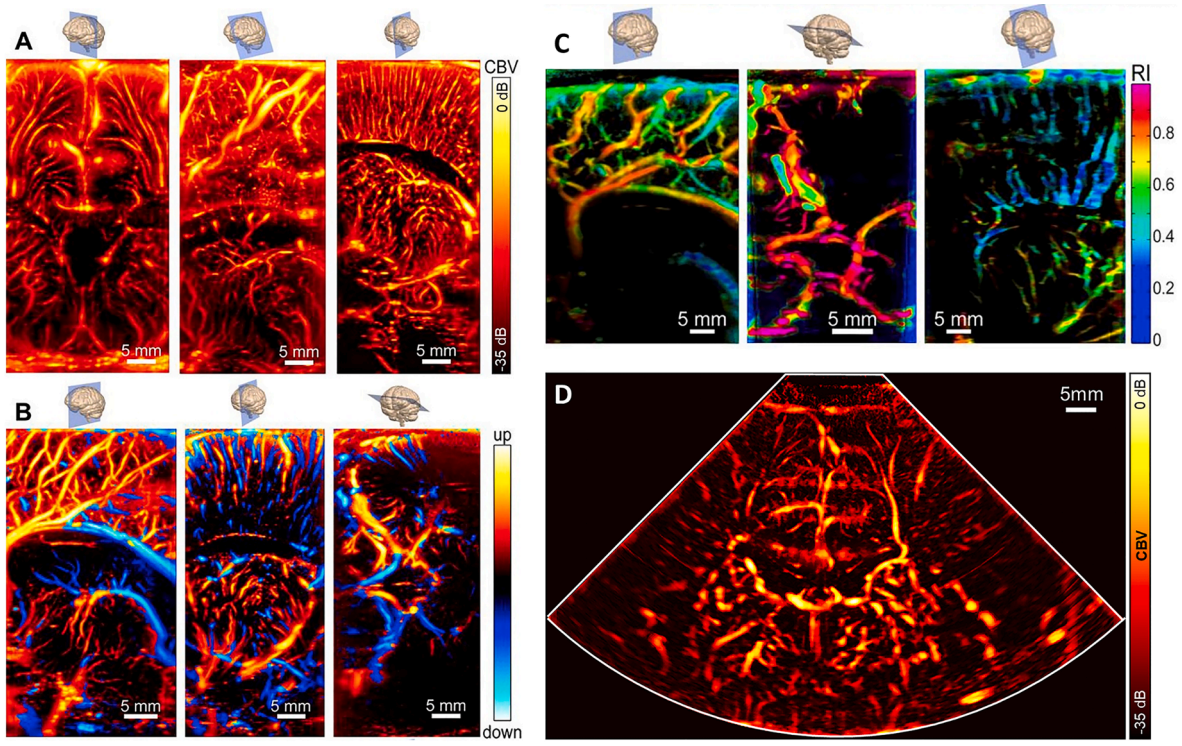

Fig. 8. Ultrafast Ultrasound Imaging (UUI). Transfontanellar Ultrafast Doppler images of a neonate's brain in different views. A: From left to right, coronal, tilted parasagittal and parasagittal views. The color scale maps the CBV using the ultrasound Power Doppler feature. B: From left to right, sagittal, parasagittal, and *trans*-temporal axial views. The Power-Doppler images include directional information (red: flow toward the probe, blue: flow away from the probe). Visible structures include pericallosal artery, veins below the cerebral ventricles, cortical penetrating arterioles and venules, and the circle of Willis. C: Vascular RI mapped in sagittal, axial, and parasagittal views. (A, B & C) Adapted and with permission from Demene et al. (Demene et al., 2019). D: Sectorial Ultrafast Doppler image obtained in coronal view. (For interpretation of the references to color in this figure legend, the reader is referred to the web version of this article.)

require trained and experienced personnel.

3.2.4. Ultrafast ultrasound imaging (UUI)

Ultrasound imaging has seen major breakthroughs in the past two decades with the advent of new technologies such as UUI. While the underlying acoustic physics are the same as in conventional ultrasound previously described in this manuscript, progress in electronics and computing have enabled the use of plane or diverging waves. These unfocused waves allow the reconstruction of an image with a single emission. Hence, the modality can reach frame rates of up to 10,000 images per second. By compounding multiple waves of different orientations, the spatial resolution is equivalent to conventional ultrasound (down to 50 μm) (Tanter and Fink, 2014). The combination of this high frame rate and high spatio-temporal resolution enables advanced signal processing strategies to image blood flows in major arteries as well as slower flows in micro-vessels (with velocities down to 1 mm/s), giving rise to Ultrafast Doppler. This modality is particularly well suited for neonates as ultrasound can penetrate deep into the brain (up to 8 cm) through the fontanelle and can be performed at bedside. As with conventional ultrasound, UUI is non-invasive and does not involve ionizing radiation. By averaging ultrafast Power Doppler images over one cardiac cycle, high-definition maps of brain vascularization were obtained by Demene et al using a linear array transducer (Fig. 8, A,B,C) (Demene et al., 2014). Sectorial images were obtained using phased-array transducer by some of the authors of this manuscript (JB, OV, JA) at The Hospital for Sick Children, Toronto, Canada (Fig. 8D).

Within the same acquisition, it is also possible to quantify blood flow within any region of interest, in terms of CBV and flow velocities. Similar to conventional Doppler (see previous section), CBV measurements are in relative units. Thus, ultrafast Doppler merges conventional Color Doppler and Pulse-Wave Doppler into a single modality. By analyzing the flow variations during the cardiac cycle, the vascular resistivity of every vessel can be assessed and mapped (Demene et al., 2014) (Fig. 8C). The first clinical applications have highlighted the potential of this method in studying neonatal brain perfusion during hypothermia in neonates with HIE (Demene et al., 2014). The analysis of flow variations during the cardiac cycle also enables the differentiation of arterial and venous flow, based on their different resistivity. Ultrafast Doppler is a promising bedside monitoring modality. With repetitive acquisition of perfusion images of the brain, neurovascular coupling can also be observed. The first application of this so-called functional ultrasound technique brought new insight into the complex subcortical and cortical hemodynamics during epileptiform seizures (Demene et al., 2017). The observed CBV spontaneous oscillations also prove to be different in thalamic and cortical areas between preterm and control term-born neonates (Baranger et al., 2021). Future development of Ultrafast Doppler implies the commercialization of dedicated scanners, as most of the current devices remain research systems. Ultimately, preclinical work demonstrated the feasibly of 3D ultrafast ultrasound, suggesting the feasibility of developing volumetric Ultrafast Doppler (Provost et al., 2015). Furthermore, using the same scanners and injected contrast agents, the spatial resolution of Ultrafast Doppler can be dramatically increased. This so-called Ultrafast ultrasound localization microscopy can delineate vessels down to 10 μm but has yet to be applied to neonatal imaging (Hingot et al., 2019).

3.3. Computed tomography (CT)

CT perfusion is the dynamic acquisition of sequential CT slices following IV administration of a bolus of iodinated contrast material (Proisy et al., 2016). A continuous scanning mode (cine-mode) is used to track the passage of the contrast bolus through the cerebral vasculature while the contrast enhancement of the tissue is depicted by a time-resolved attenuation curve. CT perfusion can provide an accurate assessment of regional cerebral blood flow (CBF), volume (CBV), and mean transit time (Krishnan et al., 2017). CBF, CBV, and mean transit time maps are interpreted using post-processing software for visual assessment and quantitative analysis. In neonates, the smaller size of the brain and the more rapid rate of blood flow are biological obstacles which hinder the implementation of CT perfusion in this age group. In addition, pediatric CT perfusion is challenged by the higher frequency of motion artifacts, the use of small intravenous catheters which limit injection rates and prolong injection times, and most importantly the concerns of ionizing radiation, which commonly require an additional 1.57 – 2.96 mSv for a CT perfusion acquisition (Nievelstein et al., 2010; Raybaud and Barkovich, 2012; Wintermark et al., 2005, 2004a). Risk-benefit considerations of ionizing radiation with CT perfusion suggest that there are very limited applications in children (Raybaud and Barkovich, 2012).

Very few CT perfusion studies have included neonates (Wintermark et al., 2005, 2004a). Wintermark et al assessed the use of CT perfusion in the emergency setting (Wintermark et al., 2005) and determined age-related variations in quantitative CT perfusion values in 77 children with an age range of 7 days to 18 years including 10 patients younger than 12 months (Wintermark et al., 2004a) (Fig. 9). CT perfusion values were consistent with other imaging techniques and showed age-specific variations with a perfusion peak around 3 years of age (Wintermark et al., 2004a).

3.4. Near-infrared spectroscopy (NIRS)

NIRS is a non-invasive imaging modality that leverages the different optical absorption properties of biological structures. Biological tissue is relatively transparent to near infrared light in the so-called optical window with wavelengths ranging from 650 to 1350 nm (Smith et al., 2009). In this same window, blood absorption strongly depends on the concentration of oxy- and deoxy-hemoglobin (Mohammadi-Nejad et al., 2018). When emitting near infrared light into cerebral tissue through the intact skull, the photons can penetrate tissue over several centimeters. Due to multiple scattering, part of this light reaches the scalp at a distant point from the emitter where it can be detected (Fig. 10). Following the Beer-Lambert law, the dynamic variations of absorption can be linked to the variations of oxy- and deoxy-hemoglobin. Based on these concentrations, NIRS provides analysis of local blood volume variations as well as oxygen consumption. Clinically, NIRS has been utilized in critical care for continuous non-invasive monitoring of regional cerebral oxygen saturation oxygenation allowing for diagnostic and therapeutic decision-making (Claessens et al., 2019; Garvey and Dempsey, 2018). One of the advantages of using NIRS is its simplicity and portability consisting in placing optical sensors or “optodes” on the neonate’s scalp at the bedside, all of which is possible given the thin skull bone and relative lack of hair.

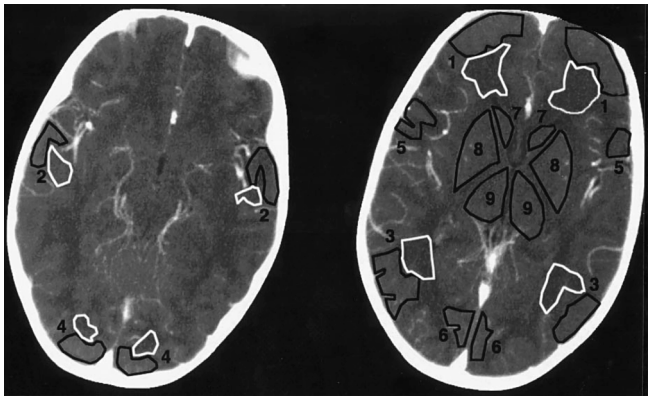

Fig. 9. Computed Tomography (CT) Perfusion. Placement of regions of interest (ROI) for regional cerebral blood volume and flow analysis within the grey (black ROIs) and white (white ROIs) matter. Adapted and with permission from Wintermark et al. (Wintermark et al., 2004b).

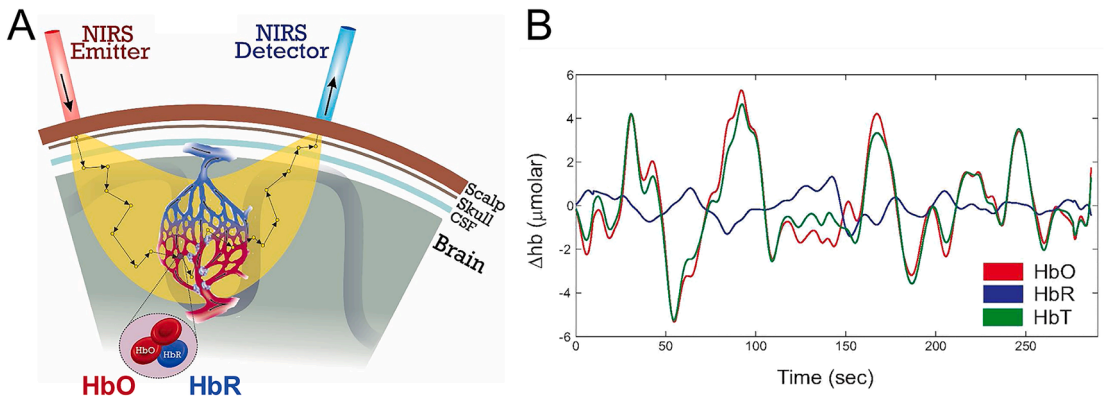

Fig. 10. A - Near-Infrared Spectroscopy principles (NIRS). An optode transmits infrared light through the scalp and skull, tissue who have limited absorption at these wavelengths. A receiving optode collects the scattered light. Adapted and with permission from Mohammadi-Nejad et al (Mohammadi-Nejad et al., 2018). B - The dynamic variations of absorption can be linked to the concentration of oxy- and deoxy-hemoglobin [HbO] and [HbR], having different absorbance properties, from which cerebral blood volume variation and oximetry is then derived. [HbT] is the total concentration of hemoglobin. Adapted and with permission from Mesquita et al. (Mesquita et al., 2010).

Combining cerebral oxygenation monitoring with arterial blood pressure is a non-invasive method that continuously estimates cerebral autoregulation and provides an opportunity to maintain stable cerebral perfusion and oxygenation during fluctuations in blood pressure (Claessens et al., 2019). Preterm neonates, infants undergoing cardiac surgery for critical congenital heart disease and those requiring extra-corporeal membrane oxygenation are at risk for acquired brain injury due to altered hemodynamics, bleeding and/or embolic phenomena. Continuous neuromonitoring for alterations in the hemodynamic status is extremely important for these neonates in an effort to identify those at higher risk for brain injury at an early stage (Claessens et al., 2019; Lin et al., 2018). NIRS was shown to be a valuable tool for continuous monitoring of cerebral oxygenation, especially for preterm infants (Hyttel-Sorensen et al., 2015) and for neonates undergoing cardiac surgery (Hirsch et al., 2009). Its temporal resolution is excellent (≈ 10 ms) compared to MRI or nuclear imaging. It is also being investigated as a promising modality for monitoring of epilepsy (Wallois et al., 2010). Furthermore, functional NIRS is an emerging neuroimaging technique capable of assessing neurovascular coupling (Mahmoudzadeh et al., 2018). Further improvements include the development of high-density (HD) optode arrays to improve spatial resolution giving rise to HD diffuse optical tomography (Singh et al., 2014). The major drawback is the poor spatial resolution, as the light path through the tissue is intrinsically unknown. Interrogation of deep structures also presents a challenge for NIRS due to the limited penetration. In-vitro experiments have shown that the typical penetration depth was 10 to 15 mm, for optodes 20 to 40 mm apart from each other (Patil et al., 2011). NIRS cannot measure absolute quantitative values of cerebral blood perfusion or oxygenation and suffers from poor reproducibility and poor inter-subject reliability. Its use should thus only be considered for monitoring purposes. Finally, there is no outcome data to date supporting the use of NIRS (Lin et al., 2018).

3.5. Nuclear imaging

Nuclear medicine approaches using either single photon emission tomography (SPECT) or positron emission tomography (PET) have been developed to image various physiological and biochemical processes within the developing brain. PET scans use radiolabeled tracers with short-lived isotopes emitting positrons which react with electrons to release high-energy gamma-rays detectable by a PET-camera (Ter-Pogossian, 1995). Local cerebral glucose metabolic rate is assessed in vivo using 2-deoxy-2[18F]-fluoro-D-glucose (FDG) (Huang et al., 1980). In contrast, SPECT uses gamma-emitting compounds, the single gamma ray detection limiting its spatial resolution (5–7 mm for SPECT compared to 3–4 mm for PET). SPECT tracers can be used for assessing cerebral blood flow.

While both PET and SPECT have been used to measure biochemical processes in children with developmental disorders, PET was also applied to the newborn population. Neonates with various types of brain injury including perinatal hypoxia–ischemia and intraventricular hemorrhage have been assessed with PET (Doyle et al., 1983) and low glucose metabolism has been shown to be associated with either reduced blood flow or delayed maturation (Suhonen-Polvi et al., 1993). PET findings during the first three weeks of life were found to correlate with amplitude integrated EEG (Thorngren-Jerneck et al., 2003) and predictive of neurodevelopmental outcome following perinatal asphyxia (Thorngren-Jerneck et al., 2001) (Fig. 11). Therapeutic hypothermia was associated with an improvement in glucose uptake (Luo et al., 2014) but further studies are required to determine the optimal timing and added-value of PET as a prognostic tool.

Generally, the role of nuclear imaging, including PET and SPECT, is very limited in neonates considering the inherent exposure to ionizing radiation. Whilst still considered relatively low, the estimated effective whole-body dose equivalent in the studies performed by Thorngren-Jerneck et al. was 0.16–0.17 mSv/MBq. Assuming a standard neonate weight of 3.5 kg (IRCP, 2002) and following weight-based radiopharmaceutical administration guidelines (Treves et al., 2016), the estimated injected activity would be 14 MBq, resulting in an effective dose of approximately 2.4 mSv.

4. Current limitations and perspectives in neonatal brain imaging

Several imaging methods exist to assess brain perfusion as summarized in Table 1. However, when imaging a neonate, safety and feasibility limit the available options. As described in this review, CT and nuclear imaging have technical advantages but their inherent risks related to exposure to ionizing radiation limit their use in neonates. On the other hand, NIRS is considered safe and easily applied at the patient's bedside, however of limited use considering its local and imperfect estimation of brain perfusion. In light of this, ultrasound and MRI currently appear to be the best suited imaging techniques to meet the constraints and specificities of neonates (see graphical abstract).

Accessibility to an MRI scanner can prove difficult due to several reasons, ranging from availability to practicability, especially when considering the critically ill neonate in the intensive care unit or in the immediate post-operative setting, where the process of transferring the patient to an MRI suite may be deemed too risky (Essig et al., 2013). Given the risks of general anesthesia, the established feed and sleep

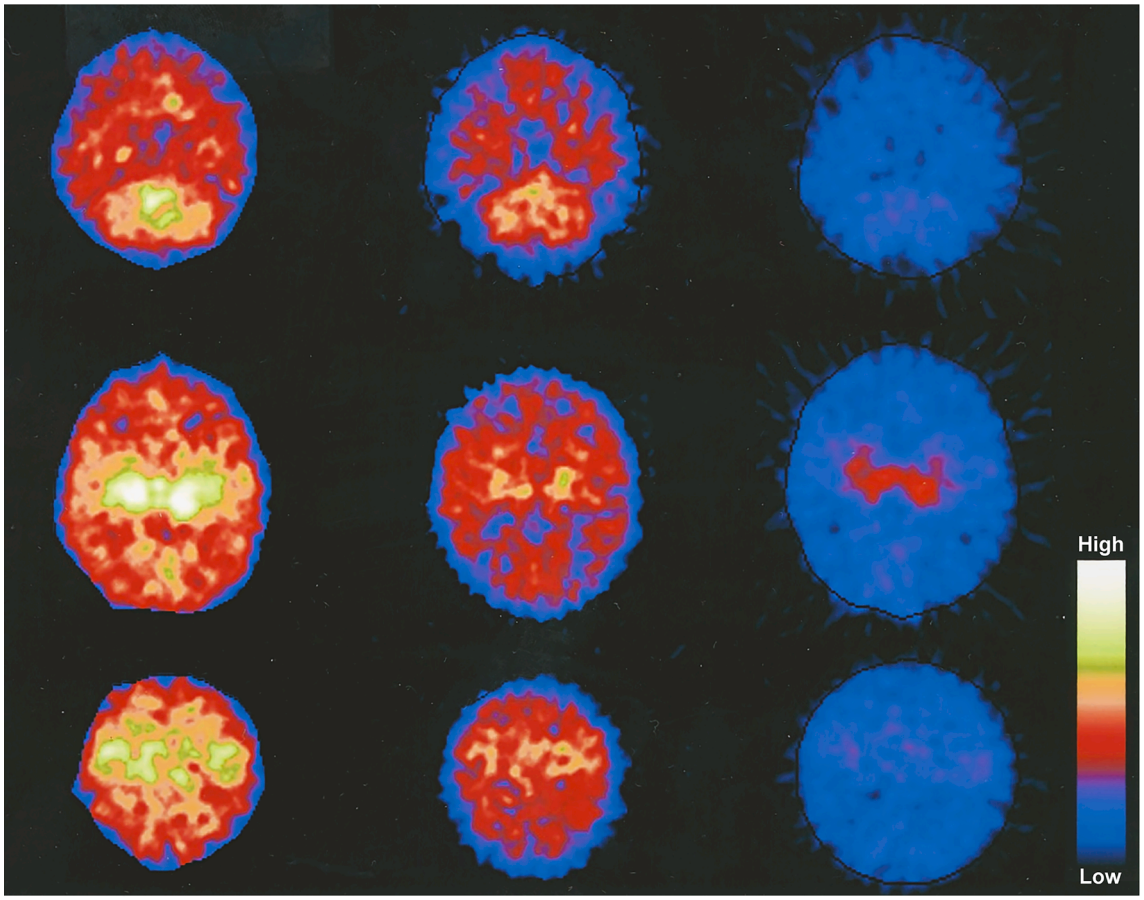

Fig. 11. Positron Emission Tomography (PET). Cerebral metabolic rate of glucose is measured in the subacute period (10 –11 days) after perinatal asphyxia in three infants (one per column) with different degrees of hypoxic-ischemic encephalopathy and shown at the level of the cerebellum (top row), thalamus (middle row), and sensorimotor cortex (bottom row). The neonate to the right has developed cerebral palsy with complicated seizures. The neonate to the left was healthy at the two-year follow-up. Adapted and with permission from Thorngren-Jerneck et al. (Thorngren-Jerneck et al., 2001).

Table 1
Imaging features of common brain perfusion imaging modalities.

		Spatial Resolution (mm)	Parameters	IV access needed	Ionizing radiation	Clinical Interests	Clinical Disadvantages
Ultrasound	**Conventional Doppler**	0.5–2	CBF	No	–	Bedside use	Operator dependent Mostly 2D
	DTPM	0.5–2	Regional perfusion intensity	No	–		
	CEUS	0.5–2	Qualitative CBF	Yes (microbubbles)	–		
	UUI	0.1–0.5	Quantitative CBF, resistivity mapping	No	–		
MRI	**DSC**	1–2	CBF, CBV, Mean transit time, Time to peak	Yes (GBCA)	–	High sensitivity, 3D	Required infrastructure, transport, support personnel and costs
	DCE		CP, CBF, CBV	Yes (GBCA)	–		
	Phase-Contrast		CBF (global only)	No	–		
	ASL		CBF	No	–		
	IVIM		CBF	No	–		
CT		0.5–0.625	CBF, CBV, Mean transit time, Time to peak	Yes (iodinated contrast)	+	Widely available, fast	Radiation, limited sensitivity
NIRS		10–20	rcSO2	No	–	Bedside use	Poor spatial resolution
Nuclear Imaging	**PET**	3–4	CBF, CBV	Yes (radiotracer)	+		High radiation
	SPECT	5–7	CBF	Yes (radiotracer)	+		

ASL: arterial spin labeling; CBF: regional cerebral blood flow; CBV: regional cerebral blood volume; CEUS: contrast enhanced ultrasound; CP: capillary permeability; CTP: computed tomography perfusion; DCE: dynamic contrast enhanced; DSC: dynamic susceptibility contrast; DTPM: dynamic tissue perfusion measurement; GBCA: gadolinium based contrast agent; IVIM: intravoxel incoherent motion; MRI: magnetic resonance imaging; NIRS: near-infrared spectroscopy; PET: positron emission tomography; rcSO2: regional cerebral oxygen saturation oxygenation; SPECT: single photon emission tomography; UUI: ultrafast ultrasound imaging.

technique is chosen as a safe and feasible alternative whenever possible (Antonov et al., 2017; Bjur et al., 2017; Heller et al., 2017; Parad, 2018). Nevertheless, this approach requires specially trained and experienced personnel (Antonov et al., 2017). Motion artifacts may limit image acquisition and may require repeating sequences.

Ultrasound imaging of the brain requires robust imaging protocols and experienced users in order to ascertain image quality and reproducibility (Dudink et al., 2020). To date, several methods have been shown to be feasible and reproducible for brain perfusion imaging in the newborn, both for global and regional applications within the brain. However, they all come with inherent limitations and challenges. When considering the volatile clinical setting of the critically ill newborn, it is important to strive for a comprehensive, but feasible approach.

5. Conclusion

Brain perfusion imaging in the neonate is gaining interest with the increasing availability of MRI perfusion sequences on modern scanners, automated post-processing methods and increasing literature supporting non-invasive methods such as ASL and IVIM MRI perfusion.

The recent advent of ultrafast doppler ultrasound imaging could represent a viable option to surmount the technical and infrastructural challenges which often render MRI impossible in the critically ill and often complex neonatal patient. Understanding the hemodynamic changes in neonates occurring around the physiological adaptation or during pathophysiological events could prove to be of paramount importance in clinical decision making and long-term outcome.

Declaration of Competing Interest

The authors declare that they have no known competing financial interests or personal relationships that could have appeared to influence the work reported in this paper.

References

ACR–ASNR–SPR, 2017. Practice Parameter For The Performance Of Intracranial Magnetic Resonance Perfusion Imaging. American College of Radiology.

Alsop, D.C., Detre, J.A., Golay, X., Gunther, M., Hendrikse, J., Hernandez-Garcia, L., Lu, H., MacIntosh, B.J., Parkes, L.M., Smits, M., van Osch, M.J., Wang, D.J., Wong, E. C., Zaharchuk, G., 2015. Recommended implementation of arterial spin-labeled perfusion MRI for clinical applications: A consensus of the ISMRM perfusion study group and the European consortium for ASL in dementia. Magn. Reson. Med. 73, 102–116. https://doi.org/10.1002/mrm.25197.

Antonov, N.K., Ruzal-Shapiro, C.B., Morel, K.D., Millar, W.S., Kashyap, S., Lauren, C.T., Garzon, M.C., 2017. Feed and Wrap MRI Technique in Infants. Clin. Pediatr. (Phila) 56, 1095–1103. https://doi.org/10.1177/0009922816677806.

Appis, A.W., Tracy, M.J., Feinstein, S.B., 2015. Update on the safety and efficacy of commercial ultrasound contrast agents in cardiac applications. Echo Res. Pract. 2, R55–62. https://doi.org/10.1530/ERP-15-0018.

Baranger, J., Demene, C., Frerot, A., Faure, F., Delanoe, C., Serroune, H., Houdouin, A., Mairesse, J., Biran, V., Baud, O., Tanter, M., 2021. Bedside functional monitoring of the dynamic brain connectivity in human neonates. Nat. Commun. 12, 1080. https://doi.org/10.1038/s41467-021-21387-x.

Benders, M.J., Hendrikse, J., De Vries, L.S., Van Bel, F., Groenendaal, F., 2011. Phase-contrast magnetic resonance angiography measurements of global cerebral blood flow in the neonate. Pediatr. Res. 69, 544–547. https://doi.org/10.1203/PDR.0b013e3182176aab.

Biagi, L., Abbruzzese, A., Bianchi, M.C., Alsop, D.C., Del Guerra, A., Tosetti, M., 2007. Age dependence of cerebral perfusion assessed by magnetic resonance continuous arterial spin labeling. J. Magn. Reson. Imaging 25, 696–702. https://doi.org/10.1002/jmri.20839.

Bjur, K.A., Payne, E.T., Nemergut, M.E., Hu, D., Flick, R.P., 2017. Anesthetic-Related Neurotoxicity and Neuroimaging in Children: A Call for Conversation. J. Child Neurol. 32, 594–602. https://doi.org/10.1177/0883073817691696.

Boudes, E., Gilbert, G., Leppert, I.R., Tan, X., Pike, G.B., Saint-Martin, C., Wintermark, P., 2014. Measurement of brain perfusion in newborns: pulsed arterial spin labeling (PASL) versus pseudo-continuous arterial spin labeling (pCASL). Neuroimage Clin 6, 126–133. https://doi.org/10.1016/j.nicl.2014.08.010.

Brody, A.S., Frush, D.P., Huda, W., Brent, R.L., American Academy of Pediatrics Section on, R., 2007. Radiation risk to children from computed tomography. Pediatrics 120, 677–682. https://doi.org/10.1542/peds.2007-1910.

Carsin-Vu, A., Corouge, I., Commowick, O., Bouzille, G., Barillot, C., Ferre, J.C., Proisy, M., 2018. Measurement of pediatric regional cerebral blood flow from 6 months to 15 years of age in a clinical population. Eur. J. Radiol. 101, 38–44. https://doi.org/10.1016/j.ejrad.2018.02.003.

Claessens, N.H.P., Jansen, N.J.G., Breur, J., Algra, S.O., Stegeman, R., Alderliesten, T., van Loon, K., de Vries, L.S., Haas, F., Benders, M., Lemmers, P.M.A., 2019. Postoperative cerebral oxygenation was not associated with new brain injury in infants with congenital heart disease. J Thorac Cardiovasc Surg 158 (867–877), e861. https://doi.org/10.1016/j.jtcvs.2019.02.106.

Davenport, M., Wang, C., Asch, D., Cavallo, J., Cohan, R., Dillman, J., Ellis, J., Forbes-Amrhein, M., Gilligan, L., Krishnamurthy, R., Krishnan, P., McDonald, R.J., McDonald, J., Murphy, B.L., Mervak, B., Newhouse, J., Pahade, J., Weinreb, J., Weinstein, S., 2021. ACR Committee on Drugs and Contrast Media. ACR Manual On Contrast Media. Available at https://www.acr.org/-/media/ACR/Files/Clinical-Resources/Contrast_Media.pdf. American College of Radiology. (Accessed April 21, 2021).

Davenport, M.S., Dillman, J.R., Cohan, R.H., Hussain, H.K., Khalatbari, S., McHugh, J.B., Ellis, J.H., 2013. Effect of abrupt substitution of gadobenate dimeglumine for gadopentetate dimeglumine on rate of allergic-like reactions. Radiology 266, 773–782. https://doi.org/10.1148/radiol.12120253.

De Vis, J.B., Petersen, E.T., de Vries, L.S., Groenendaal, F., Kersbergen, K.J., Alderliesten, T., Hendrikse, J., Benders, M.J., 2013. Regional changes in brain perfusion during brain maturation measured non-invasively with Arterial Spin Labeling MRI in neonates. Eur. J. Radiol. 82, 538–543. https://doi.org/10.1016/j.ejrad.2012.10.013.

Demene, C., Baranger, J., Bernal, M., Delanoe, C., Auvin, S., Biran, V., Alison, M., Mairesse, J., Harribaud, E., Pernot, M., Tanter, M., Baud, O., 2017. Functional ultrasound imaging of brain activity in human newborns. Sci. Transl. Med. 9 https://doi.org/10.1126/scitranslmed.aah6756.

Demene, C., Mairesse, J., Baranger, J., Tanter, M., Baud, O., 2019. Ultrafast Doppler for neonatal brain imaging. Neuroimage 185, 851–856. https://doi.org/10.1016/j.neuroimage.2018.04.016.

Demene, C., Pernot, M., Biran, V., Alison, M., Fink, M., Baud, O., Tanter, M., 2014. Ultrafast Doppler reveals the mapping of cerebral vascular resistivity in neonates. J. Cereb. Blood Flow Metab. 34, 1009–1017. https://doi.org/10.1038/jcbfm.2014.49.

Doyle, L.W., Nahmias, C., Firnau, G., Kenyon, D.B., Garnett, E.S., Sinclair, J.C., 1983. Regional cerebral glucose metabolism of newborn infants measured by positron emission tomography. Dev. Med. Child Neurol. 25, 143–151. https://doi.org/10.1111/j.1469-8749.1983.tb13737.x.

Dudink, J., Jeanne Steggerda, S., Horsch, S., eurUS.brain group, 2020. State-of-the-art neonatal cerebral ultrasound: technique and reporting. Pediatr. Res. 87, 3–12. https://doi.org/10.1038/s41390-020-0776-y.

Duncan, A.F., Caprihan, A., Montague, E.Q., Lowe, J., Schrader, R., Phillips, J.P., 2014. Regional cerebral blood flow in children from 3 to 5 months of age. AJNR Am. J. Neuroradiol. 35, 593–598. https://doi.org/10.3174/ajnr.A3728.

Ehehalt, S., Kehrer, M., Goelz, R., Poets, C., Schoning, M., 2005. Cerebral blood flow volume measurements with ultrasound: Interobserver reproducibility in preterm and term neonates. Ultrasound Med. Biol. 31, 191–196. https://doi.org/10.1016/j.ultrasmedbio.2004.10.002.

Essig, M., Shiroishi, M.S., Nguyen, T.B., Saake, M., Provenzale, J.M., Enterline, D., Anzalone, N., Dorfler, A., Rovira, A., Wintermark, M., Law, M., 2013. Perfusion MRI: the five most frequently asked technical questions. AJR Am. J. Roentgenol. 200, 24–34. https://doi.org/10.2214/AJR.12.9543.

Faingold, R., Cassia, G., Morneault, L., Saint-Martin, C., Sant'Anna, G., 2016. Basal ganglia perfusion using dynamic color Doppler sonography in infants with hypoxic ischemic encephalopathy receiving therapeutic hypothermia: a pilot study. Quant. Imaging Med. Surg. 6, 510–514. https://doi.org/10.21037/qims.2016.03.01.

Federau, C., O'Brien, K., Meuli, R., Hagmann, P., Maeder, P., 2014. Measuring brain perfusion with intravoxel incoherent motion (IVIM): initial clinical experience. J. Magn. Reson. Imaging 39, 624–632. https://doi.org/10.1002/jmri.24195.

Ferre, J.C., Bannier, E., Raoult, H., Mineur, G., Carsin-Nicol, B., Gauvrit, J.Y., 2013. Arterial spin labeling (ASL) perfusion: techniques and clinical use. Diagn Interv Imaging 94, 1211–1223. https://doi.org/10.1016/j.diii.2013.06.010.

Gaddikeri, S., Gaddikeri, R.S., Tailor, T., Anzai, Y., 2016. Dynamic Contrast-Enhanced MR Imaging in Head and Neck Cancer: Techniques and Clinical Applications. AJNR Am. J. Neuroradiol. 37, 588–595. https://doi.org/10.3174/ajnr.A4458.

Garvey, A.A., Dempsey, E.M., 2018. Applications of near infrared spectroscopy in the neonate. Curr. Opin. Pediatr. 30, 209–215. https://doi.org/10.1097/MOP.0000000000000599.

Gordon, Y., Partovi, S., Muller-Eschner, M., Amarteifio, E., Bauerle, T., Weber, M.A., Kauczor, H.U., Rengier, F., 2014. Dynamic contrast-enhanced magnetic resonance imaging: fundamentals and application to the evaluation of the peripheral perfusion. Cardiovasc Diagn Ther 4, 147–164. https://doi.org/10.3978/j.issn.2223-3652.2014.03.01.

Greisen, G., 2005. Autoregulation of cerebral blood flow in newborn babies. Early Hum Dev 81, 423–428. https://doi.org/10.1016/j.earlhumdev.2005.03.005.

Greisen, G., Vannucci, R.C., 2001. Is periventricular leucomalacia a result of hypoxic-ischaemic injury? Hypocapnia and the preterm brain. Biol. Neonate 79, 194–200. https://doi.org/10.1159/000047090.

Harvey, H.B., Gowda, V., Cheng, G., 2020. Gadolinium Deposition Disease: A New Risk Management Threat. J Am Coll Radiol 17, 546–550. https://doi.org/10.1016/j.jacr.2019.11.009.

Heck, S., Schindler, T., Smyth, J., Lui, K., Meriki, N., Welsh, A., 2012. Evaluation of neonatal regional cerebral perfusion using power Doppler and the index fractional moving blood volume. Neonatology 101, 254–259. https://doi.org/10.1159/000334648.

Heller, B.J., Yudkowitz, F.S., Lipson, S., 2017. Can we reduce anesthesia exposure? Neonatal brain MRI: Swaddling vs. sedation, a national survey. J. Clin. Anesth. 38, 119–122. https://doi.org/10.1016/j.jclinane.2017.01.034.

Hingot, V., Errico, C., Heiles, B., Rahal, L., Tanter, M., Couture, O., 2019. Microvascular flow dictates the compromise between spatial resolution and acquisition time in Ultrasound Localization Microscopy. Sci. Rep. 9, 2456. https://doi.org/10.1038/s41598-018-38349-x.

Hirsch, J.C., Charpie, J.R., Ohye, R.G., Gurney, J.G., 2009. Near-infrared spectroscopy: what we know and what we need to know–a systematic review of the congenital heart disease literature. J. Thorac. Cardiovasc. Surg. 137, 154–159. https://doi.org/10.1016/j.jtcvs.2008.08.005, 159e151-112.

Hofman, M.B.M., Rodenburg, M.J.A., Markenroth Bloch, K., Werner, B., Westenberg, J.J. M., Valsangiacomo Buechel, E.R., Nijveldt, R., Spruijt, O.A., Kilner, P.J., van Rossum, A.C., Gatehouse, P.D., 2019. In-vivo validation of interpolation-based phase offset correction in cardiovascular magnetic resonance flow quantification: a multi-vendor, multi-center study. J. Cardiovasc. Magn. Reson. 21, 30. https://doi.org/10.1186/s12968-019-0538-3.

Huang, S.C., Phelps, M.E., Hoffman, E.J., Sideris, K., Selin, C.J., Kuhl, D.E., 1980. Noninvasive determination of local cerebral metabolic rate of glucose in man. Am. J. Physiol. 238, E69–82. https://doi.org/10.1152/ajpendo.1980.238.1.E69.

Hwang, M., 2019. Introduction to contrast-enhanced ultrasound of the brain in neonates and infants: current understanding and future potential. Pediatr. Radiol. 49, 254–262. https://doi.org/10.1007/s00247-018-4270-1.

Hwang, M., Sridharan, A., Darge, K., Riggs, B., Sehgal, C., Flibotte, J., Huisman, T., 2019. Novel Quantitative Contrast-Enhanced Ultrasound Detection of Hypoxic Ischemic Injury in Neonates and Infants: Pilot Study 1. J. Ultrasound Med. 38, 2025–2038. https://doi.org/10.1002/jum.14892.

Hyttel-Sorensen, S., Pellicer, A., Alderliesten, T., Austin, T., van Bel, F., Benders, M., Claris, O., Dempsey, E., Franz, A.R., Fumagalli, M., Gluud, C., Grevstad, B., Hagmann, C., Lemmers, P., van Oeveren, W., Pichler, G., Plomgaard, A.M., Riera, J., Sanchez, L., Winkel, P., Wolf, M., Greisen, G., 2015. Cerebral near infrared spectroscopy oximetry in extremely preterm infants: phase II randomised clinical trial. BMJ 350, g7635. https://doi.org/10.1136/bmj.g7635.

IRCP, 2002. Basic anatomical and physiological data for use in radiological protection: reference values. A report of age- and gender-related differences in the anatomical and physiological characteristics of reference individuals. ICRP Publication 89. Ann ICRP 32, 5–265.

Jain, V., Duda, J., Avants, B., Giannetta, M., Xie, S.X., Roberts, T., Detre, J.A., Hurt, H., Wehrli, F.W., Wang, D.J., 2012. Longitudinal reproducibility and accuracy of pseudo-continuous arterial spin-labeled perfusion MR imaging in typically developing children. Radiology 263, 527–536. https://doi.org/10.1148/radiol.12111509.

Jakab, A., Tuura, R., Kottke, R., Kellenberger, C.J., Scheer, I., 2017. Intra-voxel incoherent motion MRI of the living human foetus: technique and test-retest repeatability. Eur Radiol Exp 1, 26. https://doi.org/10.1186/s41747-017-0031-4.

Kanda, T., Ishii, K., Kawaguchi, H., Kitajima, K., Takenaka, D., 2014. High signal intensity in the dentate nucleus and globus pallidus on unenhanced T1-weighted MR images: relationship with increasing cumulative dose of a gadolinium-based contrast material. Radiology 270, 834–841. https://doi.org/10.1148/radiol.13131669.

Kanda, T., Osawa, M., Oba, H., Toyoda, K., Kotoku, J., Haruyama, T., Takeshita, K., Furui, S., 2015. High Signal Intensity in Dentate Nucleus on Unenhanced T1-weighted MR Images: Association with Linear versus Macrocyclic Gadolinium Chelate Administration. Radiology 275, 803–809. https://doi.org/10.1148/radiol.14140364.

Kellenberger, C.J., Yoo, S.J., Buchel, E.R., 2007. Cardiovascular MR imaging in neonates and infants with congenital heart disease. Radiographics 27, 5–18. https://doi.org/10.1148/rg.271065027.

Kleinerman, R.A., 2006. Cancer risks following diagnostic and therapeutic radiation exposure in children. Pediatr. Radiol. 36 (Suppl 2), 121–125. https://doi.org/10.1007/s00247-006-0191-5.

Krishnan, P., Murphy, A., Aviv, R.I., 2017. CT-based techniques for brain perfusion. Top. Magn. Reson. Imaging 26, 113–119.

Le Bihan, D., 2019. What can we see with IVIM MRI? Neuroimage 187, 56–67. https://doi.org/10.1016/j.neuroimage.2017.12.062.

Le Bihan, D., Breton, E., Lallemand, D., Grenier, P., Cabanis, E., Laval-Jeantet, M., 1986. MR imaging of intravoxel incoherent motions: application to diffusion and perfusion in neurologic disorders. Radiology 161, 401–407. https://doi.org/10.1148/radiology.161.2.3763909.

Le Bihan, D., Turner, R., 1992. The capillary network: a link between IVIM and classical perfusion. Magn. Reson. Med. 27, 171–178. https://doi.org/10.1002/mrm.1910270116.

Lin, N., Flibotte, J., Licht, D.J., 2018. Neuromonitoring in the neonatal ECMO patient. Semin. Perinatol. 42, 111–121. https://doi.org/10.1053/j.semperi.2017.12.007.

Lotz, J., Meier, C., Leppert, A., Galanski, M., 2002. Cardiovascular flow measurement with phase-contrast MR imaging: basic facts and implementation. Radiographics 22, 651–671. https://doi.org/10.1148/radiographics.22.3.g02ma11651.

Luo, M., Li, Q., Dong, W., Zhai, X., Kang, L., 2014. Evaluation of mild hypothermia therapy for neonatal hypoxic-ischaemic encephalopathy on brain energy metabolism using (18)F-fluorodeoxyglucose positron emission computed tomography. Exp Ther Med 8, 1219–1224. https://doi.org/10.3892/etm.2014.1884.

Mahmoudzadeh, M., Dehaene-Lambertz, G., Kongolo, G., Fournier, M., Goudjil, S., Wallois, F., 2018. Consequence of intraventricular hemorrhage on neurovascular coupling evoked by speech syllables in preterm neonates. Dev Cogn Neurosci 30, 60–69. https://doi.org/10.1016/j.dcn.2018.01.001.

Massaro, A.N., Bouyssi-Kobar, M., Chang, T., Vezina, L.G., du Plessis, A.J., Limperopoulos, C., 2013. Brain perfusion in encephalopathic newborns after therapeutic hypothermia. AJNR Am. J. Neuroradiol. 34, 1649–1655. https://doi.org/10.3174/ajnr.A3422.

Mesquita, R.C., Franceschini, M.A., Boas, D.A., 2010. Resting state functional connectivity of the whole head with near-infrared spectroscopy. Biomed. Opt. Express 1, 324–336. https://doi.org/10.1364/BOE.1.000324.

Miranda, M.J., Olofsson, K., Sidaros, K., 2006. Noninvasive measurements of regional cerebral perfusion in preterm and term neonates by magnetic resonance arterial spin labeling. Pediatr. Res. 60, 359–363. https://doi.org/10.1203/01.pdr.0000232785.00965.b3.

Mohammadi-Nejad, A.R., Mahmoudzadeh, M., Hassanpour, M.S., Wallois, F., Muzik, O., Papadelis, C., Hansen, A., Soltanian-Zadeh, H., Gelovani, J., Nasiriavanaki, M., 2018. Neonatal brain resting-state functional connectivity imaging modalities. Photoacoustics 10, 1–19. https://doi.org/10.1016/j.pacs.2018.01.003.

Nardone, B., Saddleton, E., Laumann, A.E., Edwards, B.J., Raisch, D.W., McKoy, J.M., Belknap, S.M., Bull, C., Haryani, A., Cowper, S.E., Abu-Alfa, A.K., Miller, F.H., Godinez-Puig, V., Dharnidharka, V.R., West, D.P., 2014. Pediatric nephrogenic systemic fibrosis is rarely reported: a RADAR report. Pediatr. Radiol. 44, 173–180. https://doi.org/10.1007/s00247-013-2795-x.

Nievelstein, R.A., van Dam, I.M., van der Molen, A.J., 2010. Multidetector CT in children: current concepts and dose reduction strategies. Pediatr. Radiol. 40, 1324–1344. https://doi.org/10.1007/s00247-010-1714-7.

Ostergaard, L., 2005. Principles of cerebral perfusion imaging by bolus tracking. J. Magn. Reson. Imaging 22, 710–717. https://doi.org/10.1002/jmri.20460.

Paldino, M.J., Barboriak, D.P., 2009. Fundamentals of quantitative dynamic contrast-enhanced MR imaging. Magn. Reson. Imaging Clin. N. Am. 17, 277–289. https://doi.org/10.1016/j.mric.2009.01.007.

Parad, R.B., 2018. Non-sedation of the neonate for radiologic procedures. Pediatr. Radiol. 48, 524–530. https://doi.org/10.1007/s00247-017-4002-y.

Patil, A.V., Safaie, J., Moghaddam, H.A., Wallois, F., Grebe, R., 2011. Experimental investigation of NIRS spatial sensitivity. Biomed. Opt. Express 2, 1478–1493. https://doi.org/10.1364/BOE.2.001478.

Pellett, A.A., Kerut, E.K., 2004. The Doppler equation. Echocardiography 21, 197–198. https://doi.org/10.1111/j.0742-2822.2004.03146.x.

Petrella, J.R., Provenzale, J.M., 2000. MR perfusion imaging of the brain: techniques and applications. AJR Am. J. Roentgenol. 175, 207–219. https://doi.org/10.2214/ajr.175.1.1750207.

Pienaar, R., Paldino, M.J., Madan, N., Krishnamoorthy, K.S., Alsop, D.C., Dehaes, M., Grant, P.E., 2012. A quantitative method for correlating observations of decreased apparent diffusion coefficient with elevated cerebral blood perfusion in newborns presenting cerebral ischemic insults. Neuroimage 63, 1510–1518. https://doi.org/10.1016/j.neuroimage.2012.07.062.

Proisy, M., Mitra, S., Uria-Avellana, C., Sokolska, M., Robertson, N.J., Le Jeune, F., Ferré, J.-C., 2016. Brain perfusion imaging in neonates: an overview. Am. J. Neuroradiol. 37, 1766–1773.

Provost, J., Papadacci, C., Demene, C., Gennisson, J.L., Tanter, M., Pernot, M., 2015. 3-D ultrafast Doppler imaging applied to the noninvasive mapping of blood vessels in vivo. IEEE Trans. Ultrason. Ferroelectr. Freq. Control 62, 1467–1472. https://doi.org/10.1109/TUFFC.2015.007032.

Prsa, M., Sun, L., van Amerom, J., Yoo, S.J., Grosse-Wortmann, L., Jaeggi, E., Macgowan, C., Seed, M., 2014. Reference ranges of blood flow in the major vessels of the normal human fetal circulation at term by phase-contrast magnetic resonance imaging. Circ. Cardiovasc. Imaging 7, 663–670. https://doi.org/10.1161/CIRCIMAGING.113.001859.

Ranke, C., Hendrickx, P., Roth, U., Brassel, F., Creutzig, A., Alexander, K., 1992. Color and conventional image-directed Doppler ultrasonography: accuracy and sources of error in quantitative blood flow measurements. J. Clin. Ultrasound 20, 187–193. https://doi.org/10.1002/jcu.1870200305.

Raybaud, C., Barkovich, A.J., 2012. Pediatric neuroimaging. Lippincott Williams & Wilkins.

Rubin, J.M., 1994. Spectral Doppler US. Radiographics 14, 139–150. https://doi.org/10.1148/radiographics.14.1.8128046.

Rubin, J.M., Adler, R.S., Fowlkes, J.B., Spratt, S., Pallister, J.E., Chen, J.F., Carson, P.L., 1995. Fractional moving blood volume: estimation with power Doppler US. Radiology 197, 183–190. https://doi.org/10.1148/radiology.197.1.7568820.

Scholbach, T.S.J., 2009. Dynamic Sonographic Tissue Perfusion Measurement. J Med Ultrasound 17, 71–85. https://doi.org/10.1016/S0929-6441(09)60114-4.

Scholbach, T.S., J.; DiMartino, E., 2008. Dynamic Sonographic Tissue Perfusion Measurement with the PixelFlux Method. In: Hayat, M.A. (Ed.), Cancer Imaging: Lung and Breast Carcinomas, pp. 115–125.

Singh, H., Cooper, R.J., Wai Lee, C., Dempsey, L., Edwards, A., Brigadoi, S., Airantzis, D., Everdell, N., Michell, A., Holder, D., Hebden, J.C., Austin, T., 2014. Mapping cortical haemodynamics during neonatal seizures using diffuse optical tomography: a case study. Neuroimage Clin. 5, 256–265. https://doi.org/10.1016/j.nicl.2014.06.012.

Smith, A.M., Mancini, M.C., Nie, S., 2009. Bioimaging: second window for in vivo imaging. Nat. Nanotechnol. 4, 710–711. https://doi.org/10.1038/nnano.2009.326.

Spilt, A., Box, F.M., van der Geest, R.J., Reiber, J.H., Kunz, P., Kamper, A.M., Blauw, G.J., van Buchem, M.A., 2002. Reproducibility of total cerebral blood flow measurements using phase contrast magnetic resonance imaging. J. Magn. Reson. Imaging 16, 1–5. https://doi.org/10.1002/jmri.10133.

Stieb, S., Boss, A., Wurnig, M.C., Ozbay, P.S., Weiss, T., Guckenberger, M., Riesterer, O., Rossi, C., 2016. Non-parametric intravoxel incoherent motion analysis in patients with intracranial lesions: Test-retest reliability and correlation with arterial spin labeling. Neuroimage Clin 11, 780–788. https://doi.org/10.1016/j.nicl.2016.05.022.

Suhonen-Polvi, H., Kero, P., Korvenranta, H., Ruotsalainen, U., Haaparanta, M., Bergman, J., Simell, O., Wegelius, U., 1993. Repeated fluorodeoxyglucose positron

emission tomography of the brain in infants with suspected hypoxic-ischaemic brain injury. Eur. J. Nucl. Med. 20, 759–765. https://doi.org/10.1007/BF00180905.
Tanner, S.F., Cornette, L., Ramenghi, L.A., Miall, L.S., Ridgway, J.P., Smith, M.A., Levene, M.I., 2003. Cerebral perfusion in infants and neonates: preliminary results obtained using dynamic susceptibility contrast enhanced magnetic resonance imaging. Arch. Dis. Child. Fetal Neonatal Ed. 88, F525–530. https://doi.org/10.1136/fn.88.6.f525.
Tanter, M., Fink, M., 2014. Ultrafast imaging in biomedical ultrasound. IEEE Trans. Ultrason. Ferroelectr. Freq. Control 61, 102–119. https://doi.org/10.1109/tuffc.2014.2882.
Ter-Pogossian, M.M., 1995. Positron emission tomography. In: M. M.; Wagner, H.N.S., Z.; Buchanan, J. W. (Ed.). WB Saunders, London, pp. 342–346.
Thorngren-Jerneck, K., Hellstrom-Westas, L., Ryding, E., Rosen, I., 2003. Cerebral glucose metabolism and early EEG/aEEG in term newborn infants with hypoxic-ischemic encephalopathy. Pediatr. Res. 54, 854–860. https://doi.org/10.1203/01.PDR.0000088068.82225.96.
Thorngren-Jerneck, K., Ohlsson, T., Sandell, A., Erlandsson, K., Strand, S.E., Ryding, E., Svenningsen, N.W., 2001. Cerebral glucose metabolism measured by positron emission tomography in term newborn infants with hypoxic ischemic encephalopathy. Pediatr. Res. 49, 495–501. https://doi.org/10.1203/00006450-200104000-00010.
Treves, S.T., Gelfand, M.J., Fahey, F.H., Parisi, M.T., 2016. 2016 Update of the North American Consensus Guidelines for Pediatric Administered Radiopharmaceutical Activities. J. Nucl. Med. 57, 15N–18N.
Varela, M., Petersen, E.T., Golay, X., Hajnal, J.V., 2015. Cerebral blood flow measurements in infants using look-locker arterial spin labeling. J. Magn. Reson. Imaging 41, 1591–1600. https://doi.org/10.1002/jmri.24716.
Wallois, F., Patil, A., Heberle, C., Grebe, R., 2010. EEG-NIRS in epilepsy in children and neonates. Neurophysiol. Clin. 40, 281–292. https://doi.org/10.1016/j.neucli.2010.08.004.
Werner, H., dos Santos, J.R., Fontes, R., Daltro, P., Gasparetto, E., Marchiori, E., Campbell, S., 2010. Additive manufacturing models of fetuses built from three-dimensional ultrasound, magnetic resonance imaging and computed tomography scan data. Ultrasound Obstet. Gynecol. 36, 355–361. https://doi.org/10.1002/uog.7619.
Windram, J., Grosse-Wortmann, L., Shariat, M., Greer, M.L., Crawford, M.W., Yoo, S.J., 2012. Cardiovascular MRI without sedation or general anesthesia using a feed-and-sleep technique in neonates and infants. Pediatr. Radiol. 42, 183–187. https://doi.org/10.1007/s00247-011-2219-8.
Wintermark, M., Cotting, J., Roulet, E., Lepori, D., Meuli, R., Maeder, P., Regli, L., Deonna, T., Schnyder, P., Gudinchet, F., 2005. Acute brain perfusion disorders in children assessed by quantitative perfusion computed tomography in the emergency setting. Pediatr. Emerg. Care 21, 149–160.
Wintermark, M., Lepori, D., Cotting, J., Roulet, E., van Melle, G., Meuli, R., Maeder, P., Regli, L., Verdun, F.R., Deonna, T., 2004a. Brain perfusion in children: evolution with age assessed by quantitative perfusion computed tomography. Pediatrics 113, 1642–1652.
Wintermark, M., Lepori, D., Cotting, J., Roulet, E., van Melle, G., Meuli, R., Maeder, P., Regli, L., Verdun, F.R., Deonna, T., Schnyder, P., Gudinchet, F., 2004b. Brain perfusion in children: evolution with age assessed by quantitative perfusion computed tomography. Pediatrics 113, 1642–1652. https://doi.org/10.1542/peds.113.6.1642.
Wintermark, P., Moessinger, A.C., Gudinchet, F., Meuli, R., 2008a. Perfusion-weighted magnetic resonance imaging patterns of hypoxic-ischemic encephalopathy in term neonates. J. Magn. Reson. Imaging 28, 1019–1025. https://doi.org/10.1002/jmri.21525.
Wintermark, P., Moessinger, A.C., Gudinchet, F., Meuli, R., 2008b. Temporal evolution of MR perfusion in neonatal hypoxic-ischemic encephalopathy. J. Magn. Reson. Imaging 27, 1229–1234. https://doi.org/10.1002/jmri.21379.
Wu, W.C., Jiang, S.F., Yang, S.C., Lien, S.H., 2011. Pseudocontinuous arterial spin labeling perfusion magnetic resonance imaging–a normative study of reproducibility in the human brain. Neuroimage 56, 1244–1250. https://doi.org/10.1016/j.neuroimage.2011.02.080.
Young, J.R., Pope, W.B., Bobinski, M., 2018. Gadolinium Deposition within the Pediatric Brain: No Increased Intrinsic T1-Weighted Signal Intensity within the Dentate Nucleus following the Administration of a Minimum of 4 Doses of the Macrocyclic Agent Gadoteridol. AJNR Am. J. Neuroradiol. 39, 1604–1608. https://doi.org/10.3174/ajnr.A5748.